Heliyon 5 (2019) e01798

Contents lists available at ScienceDirect

Heliyon

journal homepage: www.heliyon.com

Simulated microgravity induces nuclear translocation of Bax and BCL-2 in glial cultured C6 cells

Tommaso Bonfiglio [a], Federico Biggi [h], Anna Maria Bassi [b], Sara Ferrando [c], Lorenzo Gallus [c], Fabrizio Loiacono [d], Silvia Ravera [e], Marino Rottigni [c], Sonia Scarfi [c], Felice Strollo [f], Stefania Vernazza [h], Maurizio Sabbatini [g], Maria A. Masini [g,*]

[a] Department of Internal Medicine, University of Genoa, Viale Benedetto XV 6, 16132 Genoa, Italy
[b] DIMES, University of Genoa, Viale Benedetto XV 6, 16132 Genoa, Italy
[c] DISTAV, University of Genova, Corso Europa 26, 16132 Genoa, Italy
[d] Istituto G.Gaslini, Via Gerolamo Gaslini 5, 16147 Genoa, Italy
[e] DIMES, Biochemistry Lab., University of Genoa, Viale Benedetto XV 3, 16132 Genoa, Italy
[f] Endocrinology and Diabetes Unit, St. Peter's FBF Hospital, Via Cassia 600, 00189 Rome, Italy
[g] DISIT, University of Piemonte Orientale, Via Teresa Michel 11, Alessandria, Italy
[h] University of Genova, Italy

ARTICLE INFO

Keywords:
Cell biology
Biochemistry

ABSTRACT

Alterations in the control of apoptotic processes were observed in cells during space flight or under simulated microgravity, the latter obtained with the 3D-Random Positioning Machine (3D-RPM).

Usually the proteins Bax and Bcl-2, act as pro- or anti-apoptotic regulators. Here we investigated the effects of simulated microgravity obtained by the 3D-RPM on cell viability, localization and expression of Bax and Bcl-2 in cultures of glial cancerous cells. We observed for the first time a transient cytoplasmic/nuclear translocation of Bax and Bcl-2 triggered by changing gravity vector. Bax translocates into the nucleus after 1 h, is present simultaneously in the cytoplasm after 6 h and comes back to the cytoplasm after 24 h. Bcl-2 translocate into the nucleus only after 6 h and comes back to the cytoplasm after 24 h. Physiological meaning, on the regulation of apoptotic event and possible applicative outcomes of such finding are discussed.

1. Introduction

Manned space flight and longstanding utilization of the International Space Station motivate biologists to understand whether and how microgravity (μg) represents a threaten to living organisms, including human beings. According to results obtained on astronauts, weightlessness induces a series of pathophysiological changes, some of which involving the nervous system [1, 2, 3].

Studies at the cellular level during space flight showed a series of alterations occurring in the cytoskeleton of lymphocytes and macrophages as well as in cells or tissue culture [4, 5].

In rats flown in space for 9 days, motor neurons and glial cells of anterior horns from cervical and lumbar enlargements of the spinal cord showed shape alterations and decreased cytochrome-oxidase activity providing evidence of impaired function [6]. Therefore, to understand whether μg represents a crucial factor for any organisms, it is crucial to investigate upon the biological effects of altered gravity on cells.

Due to the costs and time limitation of space flight, various methods have been used to simulate the biological effects of μg on Earth. The 3D-RPM is one of the most useful devices with respect to that. It simulates some of the physical effects of space flight by providing a vector averaged reduction (10^{-6}g) of the apparent gravity without generating significant shear forces [7]. The equipment is supplemented with a computer-assisted electronic controller driving the RPM motors according to a correct "angular walk speed". Hoson and coworkers (1997) [8] validated the 3D-RPM method by comparing the results obtained under real μg with those obtained under 3D-RPM on plant cell endoplasmic reticulum.

Takeda and coworkers (2009) [9], using three different human malignant glioma cell lines (D54MG, U251MG, T98G), demonstrated that all cancer cell lines exposed for three days to simulated microgravity shown a decrease of the cell growth, but the mechanisms of cell cycle blocked

* Corresponding author.
E-mail address: maria.masini@uniupo.it (M.A. Masini).

https://doi.org/10.1016/j.heliyon.2019.e01798
Received 30 October 2018; Received in revised form 21 February 2019; Accepted 20 May 2019

are unclear. Furthermore, in all three cell lines exposed to simulated microgravity, cytoskeleton and mitochondria changes and apoptosis increase was observed [10]. Some of us already reported upon cytoskeletal changes and apoptotic phenomena occurring in glial cells as a result of simulated μg, using 3D-RPM method [11, 12].

Mitochondrial activity is a critical point in cell surviving and physiological activity, and its functional integrity is elective site on which the apoptotic process act to induce cell to die. In particular, the relationship between apoptosis and mitochondrial activity involves two important proteins, Bax and Bcl-2. If a critical cellular condition has been reached, these proteins regulate apoptosis process by their action on mitochondria: Bcl-2 suppresses apoptosis, whereas Bax induce apoptosis: they act throughout homodimerization and heterodimerization with each other [13, 14].

Bcl-2 behaves as antiapoptotic factor in cancer cells treated by a variety of anticancer agents having as purpose to induce apoptosis. These drugs act damaging cellular microtubules by induction Bcl-2 hyperphosphorylation and reduction of Bax-Bcl-2 heterodimerization, that results in a cell block in G2 phase [15, 16]. These findings indicate a close relationship between Bcl-2 and microtubular network.

In response to apoptotic stimuli, Bax dimerizes and changes its subcellular localization moving from the cytosol to the mitochondrial membrane [17, 18]. However several studies have observed Bax nuclear translocation during apoptosis [19, 20], suggesting that Bax loses its function when is translocated into the nucleus [21].

Bcl-2 also appears overexpressed inside the nuclear compartment in HeLa cells in association with glutathione during aging and in case of oxidative stress, suggesting that some of its functions require the ability to get anchored to nucleus membranes [22, 23]. In summary, both Bcl-2 and Bax proteins have been found within the cell nucleus in various cell lines [24], suggesting that they may become a nuclear matrix-associated protein [21].

However, in simulated microgravity, the role of these two proteins, involved in the mitochondrial apoptosis, are controversial. In fact, many authors demonstrated that, in simulated microgravity, it showed a reduction BCL-2 and increment BAX gene expression in endothelial cells [25], in human osteoblastic cells [26] and in carcinoma cells [27]. Instead, other authors didn't not observed alteration between Bax-Bcl-2 ratio [28] or another found increased the level of both protein in human endothelial cells [29].

We advance the hypothesis that nucleus translocation movements of Bax and or Bcl-2, may have hidden their detection, making enigmatic the apoptotic response by simulate microgravity.

Moving on the previous findings on glial cells, in the present work, we have focused our study on C6 glioma cells as experimental in vitro model, where Bax and Bcl-2 expression and translocation by simulated microgravity was detected and analysed. A tumoral cell line was taken in account to avoid the apoptotic phenomenon of anoikis to which noncancerous cells may be subjected [30].

2. Materials and methods

Cell line. C6 glioma cells, a cell line derived from rat brain tumor kindly provided by prof. C. Pellicciari, University of Pavia, Italy, were grown in D-MEM Medium (Sigma, St. Louis, Missouri, USA) with the addition of 10% Fetal Bovine Serum, 1% Penicillin/Streptomycin and 1% Non-essential amino acids and were cultured in an incubator at the temperature of 37 °C in a humidified atmosphere containing 5% CO_2.

For experimental conditions, C6 cells were seeded, at 20.000 cells/ml using the "slide flask" method (flasks apposed onto tight-fitting removable slides, 9.0 cm^2).

Simulated Microgravity. Cells were seeded as monolayer cultures in slide flasks, which were subsequently fitted onto a special machinery called 3D Random Positioning Machine (3D RPM, Dutch Space) and kept under continuous rotation at 56°/s, at the temperature of 37 °C, for 1h, 6h and 24h (simulated μg). The flasks (completely filled with medium) are placed close to the centre of rotation to minimize centrifugal accelerations.

Frame controls (F, 1xg) were placed on the frame supporting the RPM to have the cells exposed to any vibrations eventually produced and transmitted by the rotating machinery to the supporting structure until analysed at the same time points. Another control cell group, Ground controls (g, 1xg) were kept in an incubator at 37 °C, 5% CO_2, and sham-treated in parallel, namely just kept in place until analysed at the same time points as well. At the end of each experiment, the flasks were washed with Phosphate Buffer Saline (PBS, pH 7.4) and then the cells fixed with Paraformaldehyde at 4%. Nine flasks were used to obtain cells for RT-PCR and nine flasks for Western Blot.

As F and g cell groups did not statistically differ from each other in terms of any of the parameters analysed thereafter, the paper always uses the terms "1xg" or "control" samples by referring invariably to frame controls. Having a static condition as a control group, as done in most experiments, does not allow one to separate gravitational from fluid dynamic effects.

Immunofluorescence. After being removed from flasks, the slides containing cultured cells underwent indirect immunofluorescence. After permeabilization with 0,1% Triton X-100 (Sigma in PBS, PBS washing and exposure to Normal Goat Serum (diluted 1:50 in PBS; Sigma Aldrich, St. Louis, Missouri), fixed cells were exposed at 4 °C overnight to anti-mouse Bax monoclonal antibody (mAb) (1:200 dilution; Santa Cruz Biotechnology, Dallas, Texas, U.S.A.) and anti-mouse Bcl-2 monoclonal antibody (mAb) (1:200 dilution; Santa Cruz Biotechnology) On the following day samples were washed with PBS and exposed to Alexa Fluor ® 488 (1:400 dilution; Santa Cruz Biotechnology) for 2 hours at room temperature. Immunostaining specificity was verified by omitting one of the steps of the immuno-histochemical procedure, or by replacing the primary antisera with non-immune rabbit serum or PBS.

Nuclei staining. Fixed cells were exposed to RNAse (1:500 dilution) for 15 minutes at 37 °C and then stained with propidium iodide (1:1000 dilution, stock solution 1 mg/ml) for 15 minutes at Room Temperature.

2.1. Confocal microscopy analyses

Images were obtained using a Leica TCS SL confocal microscope (Leica microsystems srl, Milan, Italy) equipped with argon/He–Ne laser sources (488, 543 and 633 nm lines) and a HCX PL APO CS 63.0 × 1.40 oil objective. During image acquisitions the 488 laser source was set at a 30% energy output and emission ranges were set between 500–550 and 600–700 nm for Alexa 488-conjugated antibodies and for propidium iodide detection, respectively. Single plane images were taken at the centre of cell thickness and pinhole was set to ensure best confocality (AU= 1 airy; m = 114.73 μm). Alternatively, stacks of 50 sections with a Z-step of 122 nm (optical thickness of each section) for a total thickness of 5.9–6 μm were taken for each image. Average projections were calculated using Leica LCS software.

2.2. Scanning electron microscope

Some of the cells were used for SEM studies. After being plated onto Leighton tubes, they were fixed in 2.5% glutaraldehyde in 0.1M cacodylate buffer, pH 7.4, for 3 h at 4 °C and identified by means of a Wild M3C stereomicroscope and a Leitz Diaplan microscope. The cells were then dehydrated in ethanol at increasing concentrations up to 100% and critical point dried with liquid CO_2 as transition fluid. The rectangular plastic pieces with the plated cells were mounted with double-sided adhesive tape on aluminum stubs and coated with a 20 nm gold layer in an argon atmosphere flow discharge sputter coating unit (Polaron E 5100). The cells were examined by an ISI SS-40 scanning electron microscope operated at an accelerating voltage of 10–20 kV.

2.3. Nuclear protein preparation

To obtain nuclear fractions, glioma C6 cells were washed in cold PBS

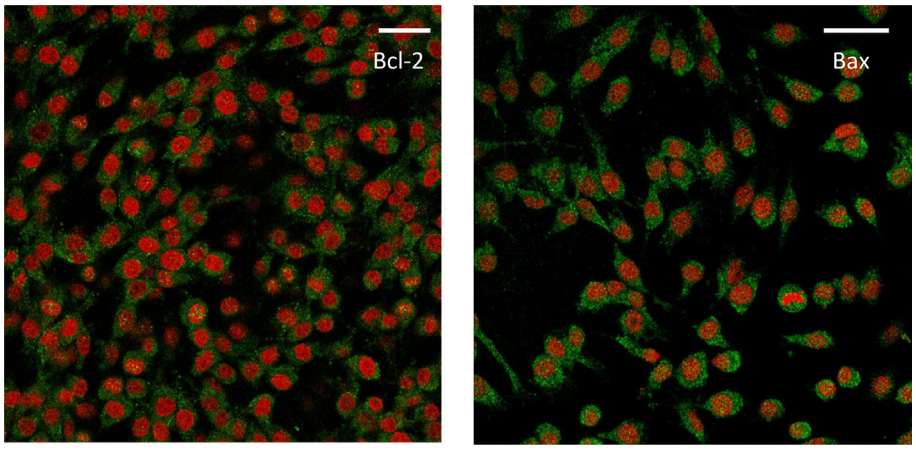

Fig. 1. Immunolocalization of Bax and Bcl-2 (green) in control cells (placed on the frame of RPM). Cells were fixed and the two proteins were stained as described under Materials and Methods. Images of representative cells with Bax and Bcl-2 localization are shown. Bax and Bcl-2 were both mainly localized only in the cytoplasm for the whole duration of the experiment but, just as an example, the figure deals with Bax at 1 h (a) and Bcl-2 at 6 h (b), for which several nuclei positive for Bax and Bcl-2 signals can be appreciated. Nuclei are stained with propidium iodide (red). Scale bar = 10μm.

and homogenated in the homogenate buffer (HB) containing: 0.25 M sucrose, 5 mM HEPES buffer, and 1 mM EDTA (pH 7.2). The samples were then centrifuged at 800x*g* for 10 min; the supernatant was discarded, and the pellet was resuspended in PBS and centrifuged at the 800x*g* for 10 min. To break nuclei, the sample was resuspended in PBS and sonicated three times for 20 sec each, in ice. Aliquots were stored at -80 °C until examined.

2.4. Mitochondria enriched-fraction isolation

Mitochondria were purified. Briefly, cells washed in PBS were homogenized in Buffer A, containing 0.25 M sucrose, 0,15 M KCl, 10 mM TRIS HCl pH 7.4, 1 mM EDTA, and 0,5% BSA. Homogenate was centrifuged at 800 g for 10 min. Supernatant was filtered (250 μm mesh filter) and centrifuged at 12000 g for 15 min. Pellet was resuspended in buffer B containing 0.25 M sucrose, 75 mM mannitol, 10 mM TRIS HCl pH 7.4, 1 mM EDTA. The final supernatant was centrifuged at 12000 g for 15 min and the mitochondrial pellet resuspended in Buffer B.

2.5. Electrophoresis, semiquantitative western blot and densitometric analysis

Denaturing electrophoresis (SDS-PAGE) was performed on gradient 10–15% acrylamide gels (SDS-PAGE). For each sample, 20 μg of total protein was loaded. The run was performed at 4 °C and at 70 mA. After blot, nitrocellulose membranes were stained with Red Ponceau, washed with Phosphate Buffer Saline (PBS) and labeled with the following primary antibodies: mouse monoclonal Ab against Bcl-2 (Santa Cruz Biotechnology; sc-509), mouse monoclonal Ab against Bax (Santa Cruz Biotechnology; sc-7480), rabbit polyclonal Ab against Adenylate Kinase isoform 1 (Sigma Aldrich), rabbit polyclonal Ab against G alpha protein (Santa Cruz Biotechnology) and goat polyclonal Ab against translocase of the inner membrane (TIM) (Santa Cruz Biotechnology; sc-17052), and goat polyclonal Ab against Laminin-B (Santa Cruz Biotechnology, CA, USA; sc-6216) all diluted in PBS +0,15% Tween (PBSt) 1:200. Bands were visualized by chemiluminescence with Immun-Star WesternC kit (BioRad Lab, CA, USA) and images were acquired with the molecular imager ChemiDoc XRS + System (Bio-Rad). Quantitative densitometry was performed using the ChemiDoc XRS + System software, and data were expressed as Relative Optical Density (R.O.D.) and are normalize against the laminin-B lane. Because in western blot analysis, the C6 cell complete homogenate was used in comparison, a further control was performed for western blot analysis against the whole protein pattern stained with Red Ponceau (data not shown). Samples Protein concentrations were determined using BSA as a standard protein.

2.6. Proliferation assay

C6 cell proliferation was also evaluated by means of DNA content. Cells were seeded in cover slides, previously put into 6-multiwell culture plates, at 30×10^3 cells density, and after 24 hours cultures were subjected to simulated μg (μg cultures) for 1h, 6h and 24h, as described above; parallel cultures were maintained in standard growth conditions, as control. At each time point, the experimental medium was removed and, after washing with warm PBS, 1 ml of lysis solution (urea 10M, 0.01% SDS in saline sodium citrate buffer [SSC] 0.154 M NaCl, 0.015 M Na_3 citrate, pH 7) was added to each sample. The dissolved cell suspensions were incubated at 37 °C in a shaking bath for 2 hours and then 1 ml of Hoechst 33258 dye, 1 mg/ml in SSC buffer, was added in the dark. Absorbance was measured with an LS5 Perkin Elmer spectrofluorometer at excitation and emission wavelengths of 355 nm and 460 nm, respectively. Cell proliferation was estimated by referring fluorescence units to a linear standard curve for DNA fluorescence versus cell number. The standard curve was performed by submitting different aliquots of C6 cells, previously counted in a haemocytometer chamber, at the same passage of those submitted to experimental procedures, then processed at the same time and conditions as experimental cultures.

2.7. Early/late apoptosis detection

Early and late apoptosis were detected by Annexin-V/PI assay; cells were stained with eBioscience Annexin V-FITC Detection Kit and evaluated for apoptosis by flow cytometry, according to the manufacturer's protocol (Bender System, Wien, Austria). C6 murine cells were washed with PBS and stained with 5 μL of annexin V-FITC in 195 μL of Binding buffer for 10 min at room temperature in the dark. Cells were then washed with PBS and resuspended in 190 μL Binding buffer and stained with 10 μL of PI before reading the sample.

Apoptotic cells were determined using the FACSCalibur equipment (Becton Dickinson), then analyzed with FlowJo, LLC. Both early apoptotic (annexin V-positive, PI-negative) and late apoptotic (annexin V-positive and PI-positive) cells were included in cell death determinations.

Experiments were performed in triplicate and result expressed as mean ± SD. Data were reported as Apoptosis index, calculated as 100 x [(treated – control)/control.

2.8. Statistical analysis

Statistical analysis was performed using ANOVA following by post hoc Bonferroni test. Normality distribution of data was assured by Kolgomorov-Smirnoff test. p values <0.05 were considered significant.

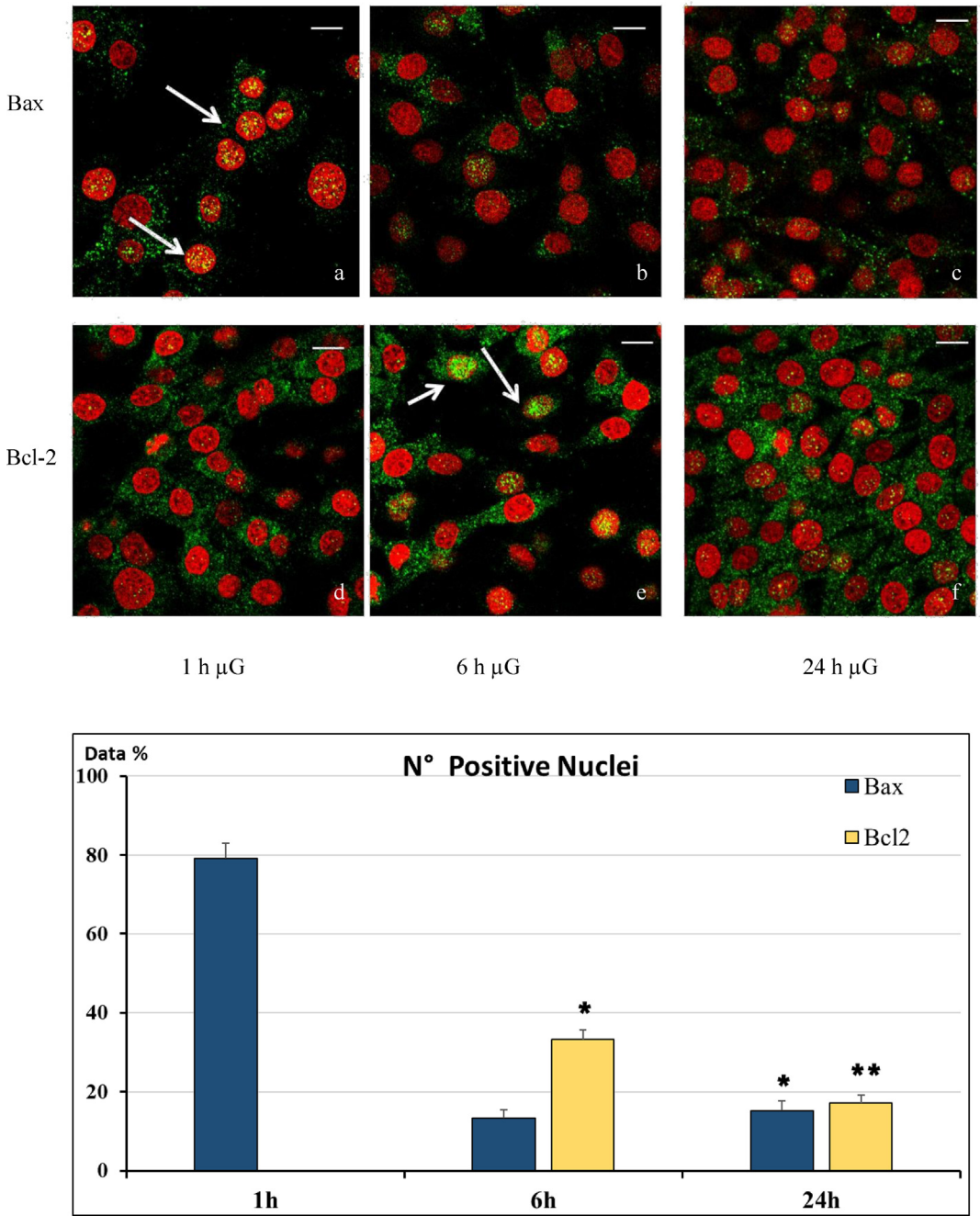

Fig. 2. Localization of Bax and Bcl-2 in C6 cells following microgravity (μg) exposition. Cells were fixed and Bax (upper panel) and Bcl-2 (lower panel) were stained as described under Materials and Methods. Images of representative cells with different Bax and Bcl-2 localization are shown. Bax is principally localized in the nucleus after 1 h of simulated microgravity (a), mainly in the cytoplasm after 6 h (b), and 24 h (c). Conversely Bcl-2 antibody staining is mostly present in the cytoplasm after 1 h (d), mostly in the nuclei after 6 h (e) and mainly in the cytoplasm after 24h (f). Nuclei are stained with propidium iodide (red). Scale bar = 10μm (g) Bar-graph showing quantitative analysis of cell nuclei positive for Bax or Bcl-2 localization. *= $p < 0.05$ vs. 1h; ** = $p < 0.05$ vs. 1h and 6h.

All statistical tests were performed by GraphPad Prism 7 software.

3. Results

3.1. Intracellular localization of Bcl-2 and Bax

C6 cells were stained with anti-Bcl-2 and Bax antibodies and examined using a laser-scanning microscope in order to get optical tomographic images at various depths within the cells.

Cells were immunostained using the above-mentioned antibodies, nuclei were marked with propidium iodide (PI) and the single images were merged to obtain both the antibody localization (green) and the nuclear staining (red) within the same picture.

Bcl-2 and Bax were localized in the cytoplasm of untreated (1xg) C6 cells during the whole duration of the experiment (Fig. 1 a,b).

In cells exposed to RPM the two proteins were visualized either in the nucleus or in the cytoplasm at different intervals: in fact, simulated μg induced a gradual translocation of Bax and Bcl-2 from the cytoplasm into the nucleus and viceversa (Fig. 2 a-f, Fig. 2g).

Bax was localized mainly in the nuclei of the cells exposed for 1 hour to simulated μg (Fig. 2a), suggesting that Bax translocated from the cytoplasm into the nucleus. However, this phenomenon was transient:

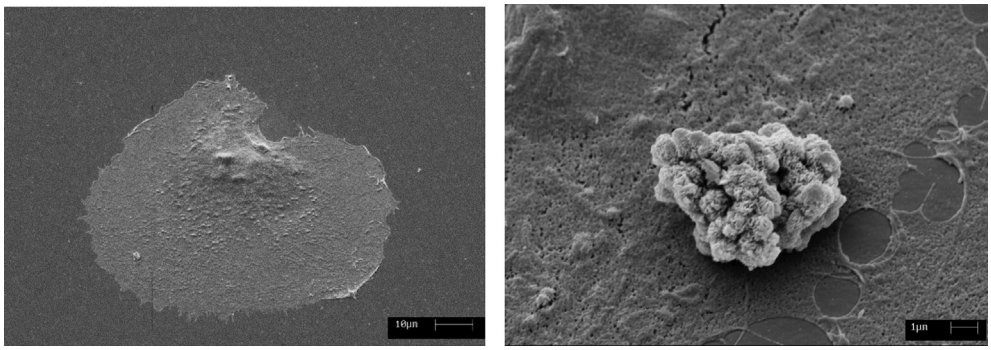

Fig. 3. SEM: Scanning Electron Microscopy micrographs of a control cell (a) and a cell exposed to simulated microgravity for 24 hours (b). The last image shows distinct morphological changes corresponding to a typical cell apoptotic feature i.e. cell membrane blebbing and background detachment.

Bax was still observed both in the cytoplasm and in the nucleus at 6 h (Fig. 2b) and mainly in the cytoplasm thereafter (Fig. 2c).

Conversely, during the course of the experiment Bcl-2 displayed a different pattern, being found mainly within the cytoplasm at 1 h from start (Fig. 2d), principally in the nucleus at 6 h from start (Fig. 2e) and mostly in the cytoplasm again after 24 h of simulated µg in almost all cells (Fig. 2f).

3.2. Scanning electron microscope (SEM) analysis

3D-RPM treatment caused cell shape changes from well flat, adherent and regular shape towards a cell morphology characterised by a ground-detached and roundish cell body, presenting numerous roundish blebs along its surface. These findings strongly address toward the interpretation of apoptotic morphology, especially evident after 24 h, as compared to control (Fig. 3).

3.3. Western immunoblotting

To confirm the data obtained by confocal microscopy, on the nuclear fraction of C6 glioma cells a Western Blot (WB) analysis was carried out.

Firstly, the nuclear fractions were characterized with several WB analysis to exclude mitochondrial or cytosolic contaminations (Fig. 4 and Supplementary 1, 2, 3, 4, 5). In particular, we employed antibodies against Adenylate kinase isoform 1 (AK1, a citosolyc protein, Supplementary 2); G alpha protein (a membrane-associated protein, Supplementary 3); TIM (a mitochondrial inner membrane translocase; Supplementary 4) and Laminin-B (a nuclear protein, Supplementary5). AK1, G alpha protein and TIM signals were detectable only in C6 cells homogenate, used as positive control, but completely absent in nuclei fractions, confirming the purity of nuclear fractions. By contrast, the signal of Laminin-B was evident in all samples, even if it appeared higher in nuclear fraction with respect the C6 cells homogenate. All data are confirmed by densitometric analysis of WB signals (Fig. 4 and Supplementary 1, 2, 3, 4, 5).

Afteward, we have evaluated the expression of Bax and Bcl-2 at different time points (1h, 6h, 24h) both at 1xG and at µG. As shown in Fig. 5 and Supplementary 6, 7, 8, Bax and Bcl-2 were well represented in isolated mitochondrial enriched fraction from control samples, whereas their signals were completely absent in nuclei extracted from control samples (Supplementary 7, 8, respectively). By contrast, the Bax signal was hugely expressed in nuclei at 1 h in µg, and then decreased at 6 h and 24 h (Supplementary 7). The Bcl-2 signal, instead, was hardly seen at 1 h in µg, peaked at 6 h and almost disappeared at 24 h (Supplementary 8). All data were confirmed by the densitometric analysis (Fig. 5).

3.4. Proliferation assay

The population doubling time of untreated C6 cultures resulted 15.02 hours, as extrapolated by DNA cellular content at T0 and 48 hours. The proliferation rate of µg cultures, instead, increased by 40% versus respective untreated cultures ($870 \pm 52 \times 10^3$ cells and $613 \pm 31 \times 10^3$ cells, respectively) after the first hour of µg, but kept stable thereafter. After 24 h µg the C6 proliferation decreased significantly up to 75%, respect untreated cultures ($860 \pm 42 \times 10^3$ and $3663 \pm 250 \times 10^3$ cells, respectively), as shown in Fig. 6.

3.5. Early/late apoptosis detection

We also investigated the apoptotic signals analyzing the Annexin-V/PI signals by cytofluorimetry.

Resuming data of AnnexinV and/or Propidium Iodide cell positivity are showed in Table 1.

Early apoptosis was immediately evident after 1h of µg exposition by an increase of Annexin-V signal over the 50% compared to control. Then the Annexin-V signal showed an exponential increase at 6 and 24h.The PI signal, evidencing the late apoptotic stage, was initially increase over 40% of the signal observed in control, but at 6h the PI signal was strongly reduced almost at level of control. Then, at 24 h the PI signal increase strongly over the 250% compared to signal detected in control. Events reported as cell Annexin-V negative and PI positive, identifying probable necrotic cell death has not revealed at significative levels and not presented in the bar-graph (Fig. 7). Although the apoptotic event is a relative fast process, the observation of a large cell apoptosis increase may be the reflex of a late activation of the apoptotic process, indicating a slow response of our experimental cell model to microgravity.

4. Discussion

In the present work microgravity application was used to investigate the effect of gravity alteration vector on cell surviving. The focus on tumor cell line assures to have cells that express surviving pathways as first line of defense in front of an environmental alteration, and not subjected to other pathways favoring cell death as mechanism to protect body organism to which the cells belong.

Our data clearly demonstrate for the first time a transient two-way nuclear/cytoplasmic Bax and Bcl-2 translocation caused by changing gravity vector.

The 3D RPM instrument used for mimic the microgavity act through a continuous rotation, obviously we can't exclude the presence of fluid motions inside the flask. Previous studies demonstrated that adherent cells less than 5% of the cell population is exposed to shear stresses greater than 50 mPa for rotational velocities up to 60 deg/s [31]. Nevertheless, RPM is an appreciated tool in microgravity-related research and is considered a valuable tool for simulating microgravity [32, 33]. In fact, using the RPM as microgravity simulator, several cell types showed similar effects as under real microgravity in space [34].

Applying microgravity to glioma cells induce Bax and Bcl-2

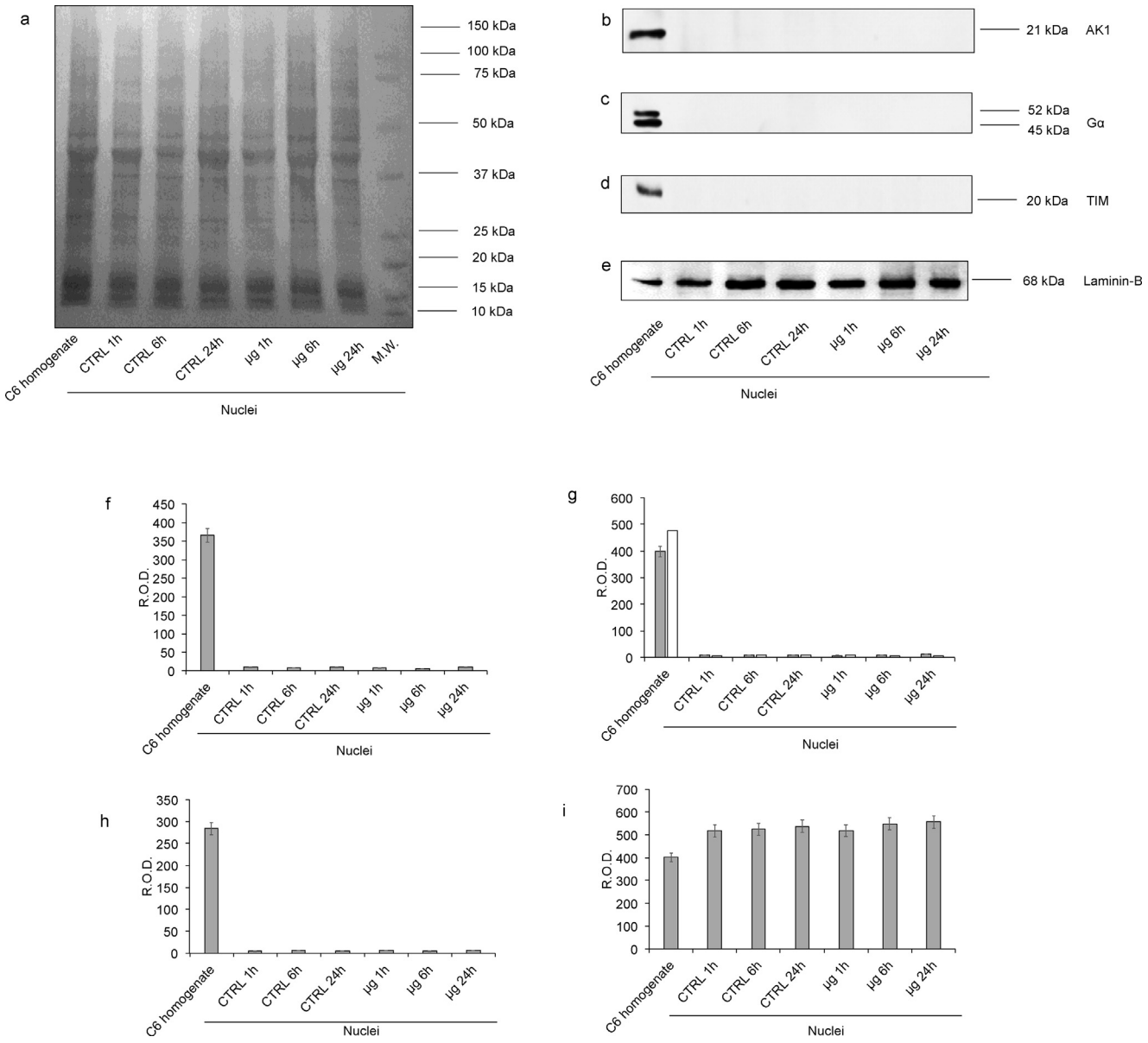

Fig. 4. Evaluation of mitochondria and plasma membrane contamination in isolated nuclei fraction by WB analysis. The figure reports the WB analyses on C6 homogenate (used as positive control) and isolated nuclei of C6 glioma cells. For each panel, the samples loaded were: lane 1, C6 glioma cells homogenate (used as control); lane 2, nuclei from untreated C6 glioma cells (time 1 hour); lane 3, nuclei from untreated C6 glioma cells (time 6 hours); lane 4, nuclei from untreated C6 glioma cells (time 24 hours); lane 5, nuclei from C6 glioma cells treated with µg for 1 hour; lane 6, nuclei from C6 glioma cells treated with µg for 6 hours; lane 7, nuclei from C6 glioma cells treated with µg for 24 hours. Panel (a) reports the protein pattern stained with Red Ponceau, full image in Supplementary section (Suppl1. F4a). Panels (b–e) show the semiquantitative results of Western Blot analysis against: Adenylate kinase isoform 1 (AK1), full image in Supplementary section (Suppl2. F4b); G protein type alpha (Gα), full image in Supplementary section (Suppl3. F4c); Translocase of the Inner Membrane (TIM), full image in Supplementary section (Suppl4. F4d). and Laminin-B full image in Supplementary section (Suppl5. F4e). The ratios of these signals were analyzed by densitometry and normalized against the protein pattern stained with Red Ponceau (f-i, respectively). The values of densitometric analysis were expressed as Relative Optical density (R.O.D.). Each panel is representative of at least five experiments and in Panels f–i data are expressed as mean ± S.D.

movements between cytoplasm and nucleus. In particular we have detected Bax translocating into nucleus after 1 h, then from there, Bax moves redistributing into nucleus and cytoplasm at 6 h, to return towards a total cytoplasmic localization following 24 h in µg.

Conversely, Bcl-2 remain in its cytoplasmic localization at 1 h in µg, then start to move into nucleus, where we can detected after 6 h of µg exposition. From nucleus Bcl-2 move back into cytoplasm, were we can detect at 24 h of µg exposition.

The analysis performed on AK1, G alpha protein and TIM, rule out any nuclear fraction contamination by elements pertaining to cytoplasm, plasma membrane or mitochondria and exclude eventual physical phenomena, like micropore formation in the nuclear membrane, caused by microgravity treatment that could allow cytoplasmic proteins transfer into the nucleus. Therefore, our data demonstrate that Bax and Bcl- 2 translocation is far from random movements and rather occurs as an independent adaptive mechanism to µg application.

Even if the apoptotic action of Bax and Bcl-2 is classically associated to their action in cytoplasm, on mitochondria integrity, the detected movements of Bax and Bcl-2 have been find associated to cell apoptosis, which morphology has been detected in the generation of blebs on the cellular surface, observed by SEM.

Apoptotic index showed an increase of apoptosis in the cells underput to µg, evidencing the occurrence of a suffering status of cellular system in µg. Moreover, the cell proliferation index, evaluated by DNA assay, in the

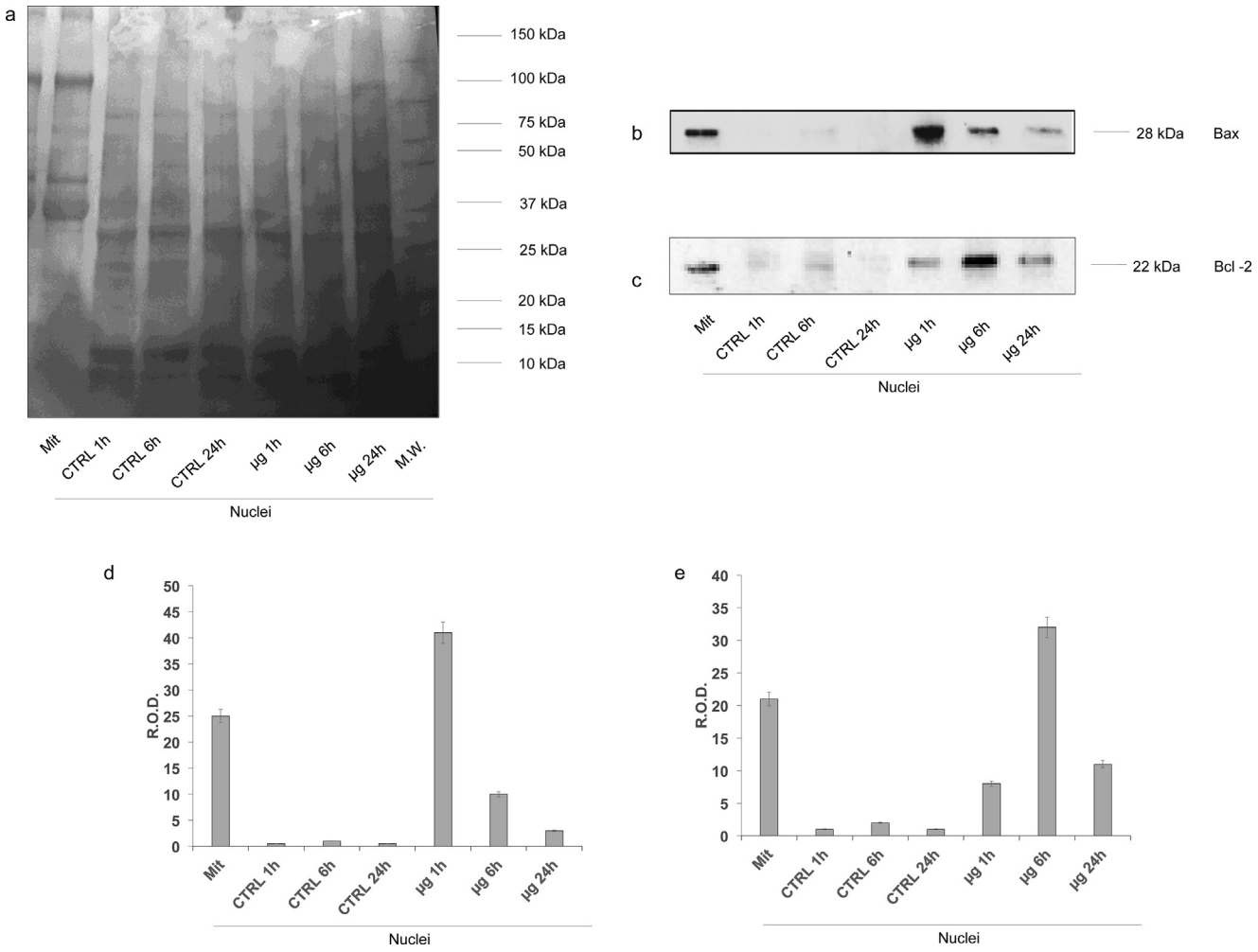

Fig. 5. Evaluation of the Bax and Bcl-2 expression in nuclear fractions by WB analysis. Figure reports the WB analyses on isolated nuclei of C6 glioma cells. For each panels, the samples loaded were: lane 1, mitochondria enriched fraction (Mit), used as positive control; lane 2, nuclei from control C6 glioma cells (time 1 hour); lane 3, nuclei from control C6 glioma cells (time 6 hours); lane 4, nuclei from control C6 glioma cells (time 24 hours); lane 5, nuclei from C6 glioma cells treated with µg for 1 hour; lane 6, nuclei from C6 glioma cells treated with µg 6 hours; lane 7, nuclei from C6 glioma cells treated with µg for 24 hours. Panel A reports the whole protein pattern stained with Red Ponceau, full image in Supplementary section (Suppl6.F5a). Panels b and c show the semiquantitative Western Blot analysis of Bax, full image in Supplementary section (Suppl7.F5b) and Bcl-2, full image in Supplementary section (Suppl8.F5c). The ratios of these signals were analyzed by densitometry and normalized against the Red Ponceau signal (Panels d and e, respectively) The values of densitometric analysis are expressed as Relative Optical density (R.O.D.). Each panel is representative of at least five experiments and in Panels d and e data are expressed as mean ± S.D.

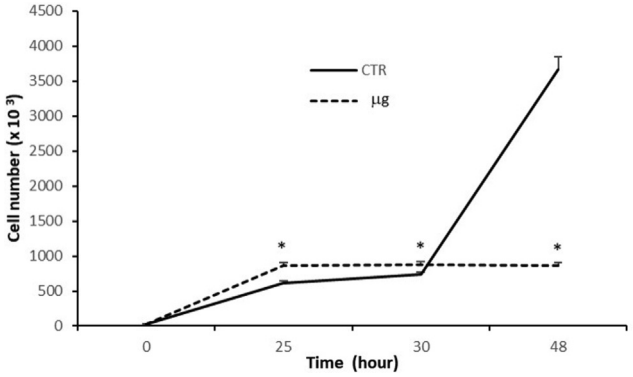

Fig. 6. Proliferation rate of C6 cells. After 24 hours from seeding C6 cells were subjected to experimental procedures, by exposure to simulated microgravity for 1, 6 and 24 hours. Untreated cultures were run and processed in parallel. Cell proliferation rate was extrapolated by referring fluorescence units to a linear standard curve for DNA fluorescence versus cell number. Data are expressed as cell number and represent the mean of 2 separate experiments, performed in triplicate ±SD. * = $p < 0.001$ vs. respective untreated cultures (ANOVA and Dunnett test). CTR = untreated cultures; µg = simulated microgravity cultures.

Table 1
Number of cells positive to AnnexinV and/or Propidium Iodide under microgravity application.

AnnexinV	Propidium Iodide	N° of cells (%)			Description
		1h	6h	24h	
+	-	9.2 ± 1.1	24.4 ± 1.9*	32.7 ± 2.8§	Early apoptosis
+	+	8.4 ± 0.9	4.1 ± 0.4*	17.6 ± 1.5§	Late apoptosis
-	+	0.5 ± 0.1	0.7 ± 0.1	1.1 ± 0.2	Necrosis
-	-	81.3 ± 5.1	71.6 ± 6.0*	48.5 ± 4.2§	Surviving cells

Data presented as Mean ± S.E.M. * = $p < 0.05$ vs. 1h; § = $p < 0.05$ vs. 1h and 6h.

same treated cells shows a parallel time-dependent reduction. For this reason, the number of apoptotic cells cannot be correlated to an increased number of cells.

However, an intriguing finding emerges from our data consisting in the different profile of the two apoptotic signals marking the so-called

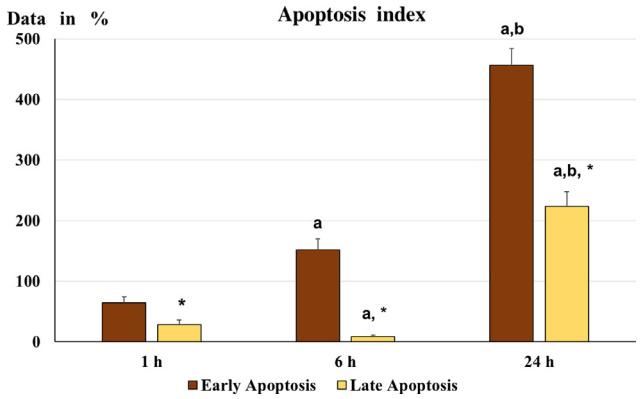

Fig. 7. Apoptotic index. The graph shows early apoptosis and late apoptosis: the data were normalized according to the Apoptosis index (calculated as 100 x [(treated – control)/control]). The higher values observed, at each time point, indicate increased apoptotic phenomena relative to controls. a= $p < 0.05$ vs. 1 h; b= $p < 0.05$ vs. 6 h; *= $p < 0.05$ vs. early apoptosis.

early apoptosis and late apoptosis.

During the apoptosis process, the cells initially express on the extracellular membrane signal such as phosphatidylserine (marked by Annexin V) identifying the so-called early apoptosis phase. During the final phase of apoptotic process (late apoptosis) the nuclear membrane integrity is loss together the DNA fragmentation allowing DNA freely available to PI staining.

In our work the early apoptosis signal showed a gradual exponential growth, confirming the occurrence of cell suffering under μg exposition. But the late apoptosis showed a signal drop just at 6 h, corresponding to time in which we have observed Bcl-2 into cell nucleus, otherwise with the exit from cell nucleus after 24 h the late apoptosis signal rapidly increases. Bcl-2 role within the nucleus is not clear, even if a possible action in regulating traffic from the cytosol to the nucleus was proposed [35], whereas Massaad et coll [22]. observed an inhibition of transcription factor activity by nuclear compartment-associated Bcl-2. These observations and our findings may indicate a novel non-canonical pathway by which Bcl-2 became a velocity controller of apoptotic process following its translocation into the nucleus.

Our works was focused on the glioma cell line because previous findings seems to indicate that mechanisms of Bax and Bcl2 nuclear translocation were active in tumoral or embryonic cell.

under particular stress conditions [35, 36], potentially identifying it as a mechanism associated to those cells that have not active the anoikis pathways, that is an apoptotic pathway typically expressed in differentiated cells [30].

In squamous carcinoma PC10 cells subjected to hyperthermia (42 °C) only Bax translocation to the nucleus was observed. The authors hypothesized it to be a mechanism acted out by those cells to escape apoptotic events; in fact this phenomenon was not observed when the same cells were treated with the chemotherapeutic agent Paclitaxel, an anticancer agent, that blocks mitosis and induces apoptosis, interacting with Bcl-2 [36]. In vivo and in vitro neonatal models also showed Bax phosphorylation and its translocation to the nucleus within few hours of hypoxic-ischemic injury in the immature brain, and a decrease of Bcl-2 and its nuclear translocation were demonstrated [37].

These findings indicate that the Bax/Bcl-2 translocation is a process used by several tumoral cell (not exposed to microgravity) identifying it as a complex pathway by which cells regulate the timing of apoptotic induction. Otherwise the alteration of cell cytoskeleton is a first evidence observed in cells exposed to microgravity [4, 12] and several authors have pointed out the link between cytoskeleton integrity and apoptosis [10, 11]. These findings may address the observed Bax/Bcl-2 translocation to cytoskeleton alteration under microgravity application.

Investigations on the effective relationships between cytoskeleton and Bax/Bcl-2 translocation deserve to be explored by use of opportune cytoskeletal blocking agents.

The evidence obtained in tumoral cells lets open the question about a real physiological role of Bax/Bcl2 nucleus translocation, but on the other hand these findings may reveal a phenomenon of apoptosis escape or slowdown performed by tumoral cells for their save and surviving. The use of other tumoral cell line and not -tumoral cells are needed to verify if these findings represent general pathways adopted by tumoral cells.

5. Conclusions

These dynamic aspects remark the occurrence of an unexpected relationship for Bax and Bcl-2 as actors involved in pathways different from that focusing on apoptotic mitochondrial destruction to which they are classically related.

The data reported in this paper, indeed suggest a possible role of these well-known cytoplasmic protein nuclear functions (transcription, mRNA stability, DNA protein scaffold stability). Future studies could be focused of temporal coordination of different cellular processes (molecular mechanisms, gene targets, macromolecular nucleoprotein complexes) occurring in distinctive cellular compartment to achieve the definitive objective (control of cell proliferation, apoptosis).

In line with other observation we observed Bax and Bcl-2 movement from cytoplasm to nucleus during response to stress that may open hypothesis on potential interaction within the nuclear compartment or introduce a role in the compartmentation or their direct action on nucleus matrix elements to realize a further regulation point along the apoptotic cascade pathway.

Of course, could be very important in order to understand the role of Bcl-2 and Bax during response to stress in particular cell types and therefore trying to understand how they move to and from the nucleus would add new knowledge on their possible, not obvious yet, interactions within the nuclear compartment.

The physiological meaning and, even more, the possible therapeutic applications of this finding could be indeed of great interest not only for researchers interested in μg but also for those working on apoptosis and cancer, because in human breast cancer cells, Bcl-2 and Bax were observed to interact within the nucleus [24].

Declarations

Author contribution statement

Tommaso Bonfiglio, Maurizio Sabbatini: Conceived and designed the experiments; Performed the experiments; Analyzed and interpreted the data; Wrote the paper.

Federico Biggi, Sara Ferrando, Felice Strollo: Conceived and designed the experiments.

Anna Maria Bassi, Silvia Ravera: Performed the experiments; Analyzed and interpreted the data; Contributed reagents, materials, analysis tools or data.

Lorenzo Gallus: Analyzed and interpreted the data.

Fabrizio Loiacono, Sonia Scarfì: Analyzed and interpreted the data; Contributed reagents, materials, analysis tools or data.

Marino Rottigni, Stefania Vernazz: Performed the experiments.

Maria A. Masin: Conceived and designed the experiments; Performed the experiments; Analyzed and interpreted the data; Contributed reagents, materials, analysis tools or data; Wrote the paper.

Funding statement

This work was supported by the Italian Space Agency (ASI) (Grant number: I/010/11/0).

Competing interest statement

The authors declare no conflict of interest.

Additional information

Supplementary content related to this article has been published online at https://doi.org/10.1016/j.heliyon.2019.e01798.

Acknowledgements

A deep gratitude goes to the beloved Prof. UVA Bianca Maria, who left each of us a deep cultural and affective inheritance of incomparable and inestimable value. Thanks to Mabi.

We are also greatly indebted to UO Immunologia, Azienda Ospedaliera Universitaria San Martino-Istituto Nazionale per la Ricerca sul Cancro (AOUSM-IST) headed by Prof. M.C. Mingari.

References

[1] T.H. Monk, D.J. Buysse, L.R. Rose, Wrist actigraphic measures of sleep in space, Sleep 22 (1999) 948–954.
[2] J.R. Lackner, P. DiZio, Human orientation and movement control in weightless and artificial gravity environments, Exp. Brain Res. 130 (2000) 2¬26.
[3] K. Tanaka, T.M. Gotoh, C. Awazu, H. Morita, Roles of the vestibular system in controlling arterial pressure in conscious rats during a short period of microgravity, Neurosci. Lett. 397 (2006) 40–43.
[4] M.L. Lewis, J.L. Reynolds, L.A. Cubano, J.P. Hatton, B.D. Lawless, E.H. Piepmeier, Spaceflight alters microtubules and increases apoptosis in human lymphocytes (Jurkat), FASEB J. 12 (1998) 1007–1018.
[5] I. Walther, A. Cogoli, P. Pippia, M.A. Meloni, G. Cossu, M. Cogoli, et al., Human immuno cells as space travellers, Eur. J. Med. Res. 4 (1999) 361–363.
[6] I.V. Poliakov, O. Louri, V.R. Edzherton, I.B. Krasnov, Histochemistry and morphology of the anterior horns of spinal cord in rats after 9-day space flight, Aviakosm. Ekolog. Med 29 (1995) 30—32.
[7] A.G. Borst, J.J.W.A. van Loon, Technology and developments for the random positioning machine, RPM. Microgravity Science and Technology 21 (4) (2009) 287–292.
[8] T. Hoson, S. Kamisaka, Y. Masuda, M. Yamashita, B. Bachen, Evaluation of the three dimensional clinostat as a simulator of weightlessness, Plants 203 (1997) 187–197.
[9] M. Takeda, T. Magaki, T. Okazaki, Y. Kawahara, T. Manabe, L. Yuge, K. Kurisu, Effects of simulated microgravity on proliferation and chemosensitivity in malignant glioma cells, Neurosci. Lett. 463 (2003) 54–59.
[10] H. Schatten, M.L. Lewis, A. Chakrabarti, Spaceflight and clinorotation cause cytoskeleton and mitochondria changes and increases in apoptosis in cultured cells, Acta Astronaut. 49 (2001) 399–418.
[11] B.M. Uva, M.A. Masini, M. Sturla, F. Bruzzone, M. Giuliani, G. Tagliafierro, et al., Microgravity-induced apoptosis in cultured glial cells, Eur. J. Histochem. 46 (2002a) 209–214.
[12] B.M. Uva, M.A. Masini, M. Sturla, P. Prato, M. Passalacqua, M. Giuliani, et al., Clinorotation-induced weightlessness influences the cytoskeleton of glial cells in culture, Brain Res. 934 (2002b) 132–139.
[13] C. Wang, R.J. Youle, The role of mitochondria in apoptosis, Annu. Rev. Genet. 43 (2009) 95–118.
[14] K.J. Campbell, S.W.G. Tait, Targeting BCL-2 regulated apoptosis in cancer, Open Biol 8 (2018) 180002.
[15] S. Haldar, A. Basu, C.M. Croce, Bcl2 is the guardian of microtubule integrity, Cancer Res. 57 (1997) 229–233.
[16] R.K. Srivastava, A.R. Srivastava, S.J. Korsmeyer, M. Nesterova, Y.S. Cho-Chung, D.L. Longo, Involvement of microtubules in the regulation of Bcl-2 phosphorylation and apoptosis through cyclic AMP-dependent protein kinase, Mol. Cell. Biol. 18 (1998) 3509–3517.
[17] I.S. Goping, A. Gross, J.N. Lavoie, M. Nguyen, R. Jemmerson, K. Roth, et al., Regulated targeting of BAX to mitochondria, J. Cell Biol. 143 (1998) 207–215. PMCID: PMC2132805.
[18] M. Gill, J.R. Perez-Polo, Bax shuttling after rotenone treatment of neuronal primary cultures: effects on cell death phenotypes, J. Neurosci. Res. 87 (2009) 2047–2065. PMCID: PMC 19224578.
[19] M. Mandal, L. Adam, J. Mendelsohn, R. Kumar, Nuclear targeting of Bax during apoptosis in human colorectal cancer cells, Oncogene 17 (1998) 999–1007.
[20] B. Gajkowska, U. Wojewodzka, J. Gajda, Translocation of Bax and Bid to mitochondria, endoplasmic reticulum and nuclear envelope: possible control points in apoptosis, J. Mol. Histol. 35 (2004) 11–19.
[21] L. Lindenboim, E. Ferrando-May, C. Borner, R. Stein, Non-canonical function of Bax in stress-induced nuclear protein redistribution, Cell. Mol. Life Sci. 70 (2013) 3013–3027.
[22] C.A. Massaad, B.P. Portier, G. Taglialatela, Inhibition of transcription factor Activity by nuclear compartment-associated bcl-2, J. Biol. Chem. 279 (2004) 54470–54478.
[23] B.P. Portier, G. Taglialatela, Bcl-2 localized at the nuclear compartment induces apoptosis after transient overexpression, J. Biol. Chem. 281 (2006) 40493–40502.
[24] R.W.M. Hoetelmans, Nuclear partners of bcl-2: Bax and PML, DNA Cell Biol. 23 (2004) 351–354.
[25] C.Y. Kang, L. Zou, M. Yuan, Y. Wang, T.Z. Li, Y. Zhang, J.F. Wang, Y. Li, X.W. Deng, C.T. Liu, Impact of simulated microgravity on microvascular endothelial cell apoptosis, Eur. J. Appl. Physiol. 111 (2011) 2131–2138.
[26] H. Nakamura, Y. Kumei, S. Morita, H. Shimokawa, K. Ohya, K. Shinomiya, Antagonism between apoptotic (Bax/Bcl-2) and anti-apoptotic (IAP) signals in human osteoblastic cells under vector-averaged, Ann. N. Y. Acad. Sci. 1010 (2003) 143–147. PMID:15033709.
[27] P. Kossmehl, M. Shakibaei, A. Cogoli, M. Infanger, F. Curcio, J. Schönberger, C. Eilles, J. Bauer, H. Pickenhahn, G. Schulze-Tanzil, M. Paul, D. Grimm, Weightlessness induced apoptosis in normal thyroids cells and papillary thyroid carcinoma cells via extrinsic and intrinsic pathways, Endocrinology 144 (2003) 4172–4179.
[28] N. Rucci, S. Migliaccio, B.M. Zani, A. Taranta, A. Teti, Characterization of the osteoblast-like cell phenotype under microgravity conditions in the NASA-approved Rotating Wall Vessel bioreactor (RWV), J. Cell. Biochem. 85 (2002) 167–179.
[29] M. Infanger, P. Kossmehl, M. Shakibaei, S. Baatout, A. Witzing, J. Grosse, J. Bauer, A. Cogoli, S. Faramarzi, H. Derradji, M. Neefs, M. Paul, D. Grimm, Induction of three-dimensional assembly and increase in apoptosis of human endothelial cells by simulated microgravity: impact of vascular endothelial growth factor, Apoptosis 11 (2006) 749–764.
[30] C. Bozzo, M. Sabbatini, R. Tiberio, V. Piffanelli, C. Santoro, M. Cannas, Activation of caspase-8 triggers anoikis in human neuroblastoma cells, Neurosci. Res. 56 (2006) 145–153.
[31] S.L. Wuest, P. Stern, E. Casartelli, M. Egli, Fluid dynamics appearing during simulated microgravity using random positioning machines, PLoS One 12 (1) (2017), e0170826.
[32] S. Brungs, M. Egli, S.L.M. Wuest, P.C.W.A. Christianen, J.J. van Loon, T.J. Ngo Anh, et al., Facilities for simulation of microgravity in the ESA ground-based facility programme, Microgravity Sci. Technol. (2016) 1±13.
[33] R. Herranz, M.A. Valbuena, A. Manzano, K.Y. Kamal, F.J. Medina, Use of microgravity simulators for plant biological studies, Methods Mol. Biol. 1309 (2015) 239–254.
[34] S.L. Wuest, S. Richard, S. Kopp, D. Grimm, M. Egli, Simulated microgravity: critical review on the use of random positioning machines for mammalian cell culture, BioMed Res. Int. (2015) 971474.
[35] C. Zhu, U. Hallin, Y. Ozaki, R. Grandér, K. Gatzinsky, B.A. Bahr, et al., Nuclear translocation and calpain-dependent reduction of Bcl-2 after neonatal cerebral hypoxia-ischemia, Brain Behav. Immun. 24 (2010) 822–830.
[36] A.E. Salah-Eldin, S. Inoue, S. Tsukamoto, H. Aoi, M. Tsuda, An association of Bcl-2 phosphorylation and Bax localization with their function after hyperthermia and paclitex treatment, Int. J. Cancer 103 (2003) 53–60.
[37] S.K. Infante, A.F. Oberhauser, J.R. Perez-Polo, Bax phosphorylation association with nucleus and oligomerization after neonatal hypoxia-ischemia, J. Neurosci. Res. 91 (2013) 1152–1164.